Theoretical design of ferritic creep resistant steels using neural network, kinetic, and thermodynamic models

F. Brun, T. Yoshida, J. D. Robson, V. Narayan, H. K. D. H. Bhadeshia, and D. J. C. MacKay

A neural network model has been developed on the basis of published experimental data. This allows the creep rupture strength of bainitic and martensitic electric power plant steels with compositions based on Fe–2·25Cr–1Mo and Fe–(9–12)Cr to be estimated as a function of chemical composition, heat treatment and time at temperature. This model, together with a variety of thermodynamic and kinetic calculations, has been used to propose two new alloys related to the 10CrMoW steel which in theory have outstanding creep rupture properties. *MST/3920*

Mr Brun is in the Ecole Polytechnique, Departement de Mecanique, Paris, France, Dr Yoshida is with Ishikawajima-Harima Heavy Industries Co. Ltd, Tokyo 135, Japan, Dr Robson, Dr Narayan, and Dr Bhadeshia are in the Department of Materials Science and Metallurgy, University of Cambridge, Pembroke Street, Cambridge CB2 3QZ, UK, and Dr MacKay is in the Cavendish Laboratory, University of Cambridge, Madingley Road, Cambridge CB3 0HE, UK. *Manuscript received 4 September 1997; accepted 2 July 1998.*

Introduction

Creep resistant ferritic steels based on Fe–2·25Cr–1Mo and Fe–(9–12)Cr have been used extensively in the energy and petrochemical industries for more than half a century. This is because they have an outstanding record of reliability in quite aggressive conditions over time periods as long as 30 years. The alloys have undergone progressive development throughout their history,[1,2] particularly in order to permit the use of higher steam temperatures in power plant which can then operate with greater efficiency.

The basic principles of alloy design for creep resistance are therefore well established and well founded on experience. The steels must have a stable microstructure which contains fine alloy carbides which resist the motion of dislocations; however, changes are inevitable over the long service time so that there must be sufficient solid solution strengthening to ensure long term creep deformation. There may be other requirements such as weldability, and corrosion and oxidation resistance. It is nevertheless difficult to express the design process quantitatively given the large number of interacting variables. It was the purpose of the present work to encrypt some of the published experimental data into a quantitative procedure for estimating the creep rupture stress of power plant steels as a function of the chemical composition, heat treatment, temperature, and time. The rupture stress is chosen as the variable to model because of the ready availability of data in the open literature, and because it is a very common parameter used in industry during alloy development. The model which is developed is then tested against known metallurgical trends and used to propose two new alloys which ought to have better properties than anything developed to date. We begin with a brief description of the neural network method used to develop the quantitative model. The method used here is due to MacKay;[3–6] and it has been recently reviewed.[7]

Analysis technique

In regression analysis, data are best fitted to a specified relationship which is usually linear. The result is an equation in which each of the inputs x_j is multiplied by a weight w_j. The sum of all such products and a constant θ then gives an estimate of the output

$$y = \sum_j w_j x_j + \theta \quad . . . . . (1)$$

It is well understood that there are dangers in using such relationships beyond the range of fitted data.

A neural network is a much more general method of regression analysis. As before, the input data x_j are multiplied by weights, but the sum of all these products forms the argument of a hyperbolic tangent. The output y is therefore a non-linear function of x_j, the function usually chosen being the hyperbolic tangent because of its flexibility.[3–7] The exact shape of the hyperbolic tangent can be varied by altering the weights (Fig. 1*a*). Further degrees of non-linearity can be introduced by combining several of these hyperbolic tangents (Fig. 1*b*), so that the neural network method is able to capture almost arbitrarily non-linear relationships. It is well known that the effect of chromium on the microstructure of steels is quite different at large concentrations than in dilute alloys.[8] Ordinary regression analysis cannot cope with such changes in the form of relationships.

A neural network is 'trained' on a set of examples of input and output data. The outcome of the training is a set of coefficients (weights) and a specification of the functions which in combination with the weights relate the input to the output. The training process involves a search for the optimum non-linear relationship between the input and the output data and is computer intensive. Once the network is trained, estimation of the outputs for any given inputs is very rapid.

One of the difficulties with blind data modelling is that of 'overfitting', in which spurious details and noise in the training data are overfitted by the model (Fig. 2). This gives rise to solutions that generalise poorly. MacKay[7] has developed a Bayesian framework for neural networks in which the appropriate model complexity is inferred from the data.

The Bayesian framework for neural networks has two further advantages. First, the significance of the input variables is automatically quantified. Consequently the significance perceived by the model of each input variable can be compared against metallurgical theory, where such theory is known. Second, the network's predictions are accompanied by error bars which depend on the specific position in input space. These quantify the model's certainty about its predictions.

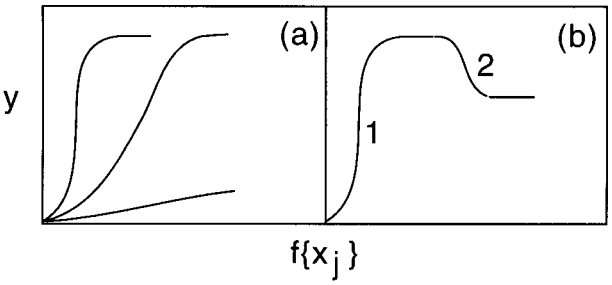

1 *a* three different hyperbolic tangent functions – 'strength' of each depends on the weights, and *b* combination of two hyperbolic tangents to produce more complex model

Database

The database compiled from the published literature[9–36] consisted of 2066 combinations of creep rupture stress and, originally, 30 inputs including the time to rupture, chemical composition, and heat treatment (Table 1). It is emphasised that the data set consisted mainly of Fe–2·25Cr–1Mo (referred to generally in this paper as 2·25Cr–1Mo type steel) and Fe–(9–12)Cr type steels because these have been extensively reported in the literature. Many of the steels were given three different heat treatments, described as normalising, tempering, and annealing, and given in that sequence. Each heat treatment can be described with three variables: the temperature, duration, and the cooling rate from the treatment temperature. There are four descriptions of this cooling rate: furnace, air, or oil or water quenching. Each of these was represented as a single variable with a value 0 or 1, the latter if the treatment was applied. Four variables are therefore needed to represent the cooling rate, for example with values 0, 1, 0, 0 for air cooling. In some cases the steel had only two heat treatments in which case the third temperature, duration, and cooling rate columns were all set to zero. The time to rupture was expressed in logarithmic form since the rupture stress in creep theory varies with the logarithm of time. The rupture stress was modelled as a function of all the other variables including time because it always has finite values whereas the time can become infinitely large as the stress decreases. A well behaved function is necessary for the neural network analysis.[7]

Table 1 Some variables included in the data set

Variable	Range	Mean	Standard deviation
Log (creep rupture time)	−0·22 to 5·28	3·021	1·009
Test temperature, K	723–977	866·6	61·6
Normalising temperature, K	1123–1453	1279	70·42
Duration, h	0·17–33	2·007	3·85
Tempering temperature, K	823–1133	980	71·8
Duration, h	0·5–32	3·34	5·88
Annealing temperature, K	0–1023	230·7	404·3
Duration, h	0·5–50	3·96	8·15
Chemical composition, wt-%			
C	0·004–0·23	0·112	0·044
Si	0·01–0·86	0·29	0·17
Mn	0·27–0·92	0·51	0·11
P	0·001–0·029	0·013	0·0076
S	0·001–0·02	0·0076	0·0047
Cr	2·17–12·9	8·43	3·28
Mo	0·04–2·99	0·89	0·513
W	0·01–3·93	0·41	0·749
Ni	0·01–2·0	0·24	0·28
Cu	0·01–0·87	0·074	0·102
V	0·01–0·28	0·119	0·1
Nb	0·005–0·312	0·036	0·047
N	0·001–0·165	0·031	0·0273
Al	0·001–0·057	0·012	0·012
B	0·0003–0·051	0·001	0·004
Co	0·008–2·5	0·092	0·334
Ta	0·0003–0·1	0·0008	0·0069
O	0·003–0·035	0·0104	0·0026
Re	0·0003–0·6	0·0032	0·0416

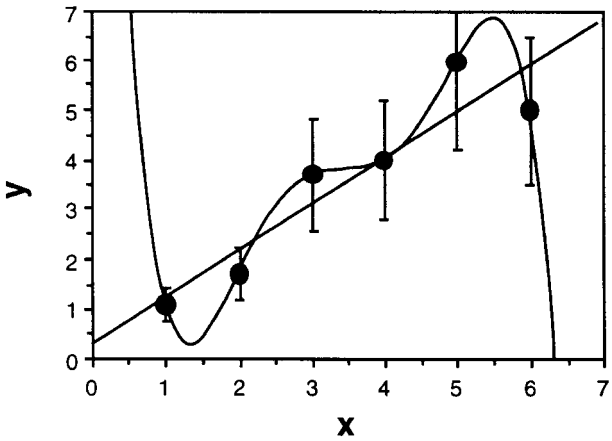

2 Complex model shown may fit data, but in this instance a linear relationship may be all that is justified by noise in data

Analysis

The aim of the present work was to predict creep rupture stress as a function of the variables listed in Table 1. Both the input and output variables were first normalised within the range $\pm 0{\cdot}5$ as follows

$$x_{\mathrm{N}} = \frac{x - x_{\min}}{x_{\max} - x_{\min}} - 0{\cdot}5 \quad \ldots\ldots\ldots\ldots (2)$$

where x_{N} is the normalised value of x which has maximum and minimum values given by $x_{\max}$ and $x_{\min}$ respectively. The normalisation is not in principle necessary but does permit the variables to be compared more readily.

The network consisted of 37 input nodes (one for each variable), a number of hidden nodes, and an output node representing the rupture stress (Fig. 3). The hidden nodes are where the mathematical operations described below are carried out. A larger number of hidden nodes represents a more complex model. The network was trained using a randomly chosen 1033 of the examples from a total of 2066 available, the remaining 1033 examples being used as 'new' experiments to test the trained network.

Linear functions of the inputs x_{j} are operated on by a hyperbolic tangent transfer function

$$h_{\mathrm{i}} = \tanh\left(\sum_{\mathrm{j}} w_{\mathrm{ij}}^{(1)} x_{\mathrm{j}} + \theta_{\mathrm{i}}^{(1)} \right) \quad \ldots\ldots\ldots\ldots (3)$$

so that each input contributes to every hidden unit. The bias is designated θ_{i} and is analogous to the constant that appears in linear regression (e.g. equation (1)). The strength of the transfer function is in each case determined by the

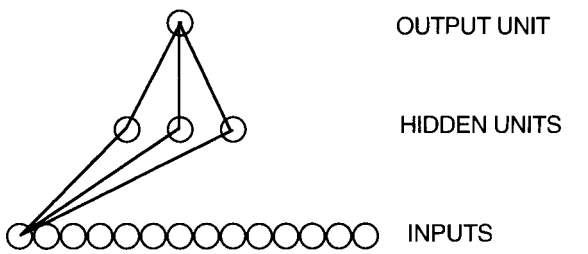

3 Typical network used in the analysis: connections originating from only one input unit are illustrated and two bias units are not illustrated

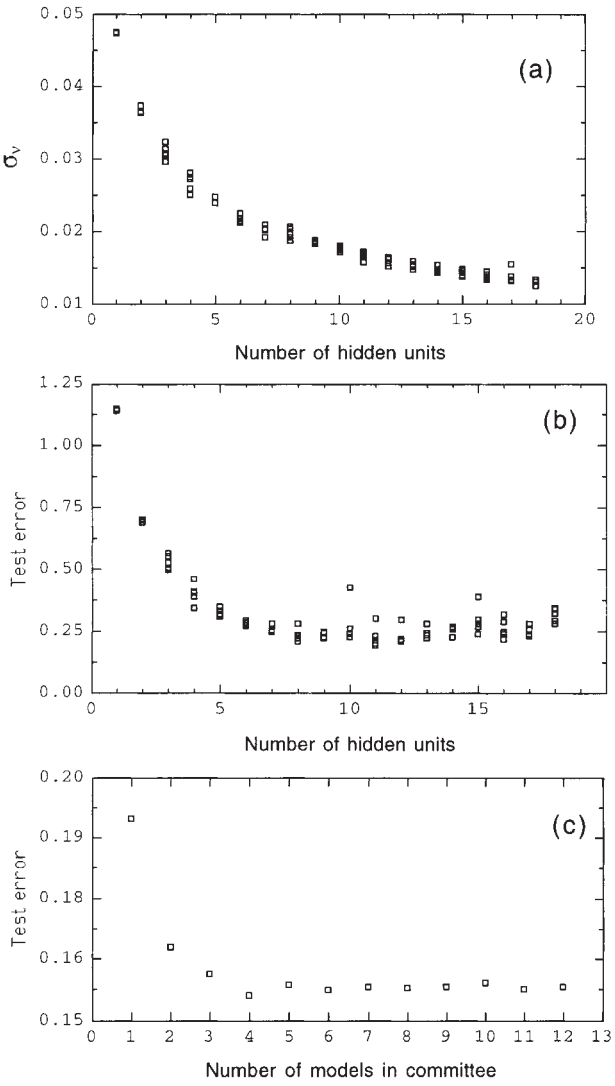

4 *a* variation in σ_v (the model perceived level of noise in the data) as function of number of hidden units: several values are presented for each set of hidden units because the training for each network was started with a variety of random seeds; *b* test error as function of number of hidden units; *c* test error as function of number of models in the committee of models

weight w_{ij}. The transfer to the output y is linear

$$y = \sum_i w_{ij}^{(2)} h_i + \theta^{(2)} \quad . \quad . \quad . \quad . \quad . \quad . \quad . \quad . \quad . \quad . \quad . \quad . \quad (4)$$

The specification of the network structure, together with the set of weights, is a complete description of the formula relating the inputs to the output. The weights are determined by training the network; the details are described elsewhere.[7] The training involves a minimisation of the regularised sum of squared errors. The term σ_v used below is the framework estimate of the noise level of the data.

The complexity of the model is controlled by the number of hidden units (Fig. 3), and the values of the 39 regularisation constants σ_w, one associated with each of the 37 inputs, one for biases, and one for all weights connected to the output.

The results of the training are presented in Fig. 4*a* which shows the model perceived noise σ_v in the training data as a function of the complexity of the model. This naturally decreases as the model becomes more flexible with increasing complexity but as discussed earlier, an over complex model may not be justified. To select the correct

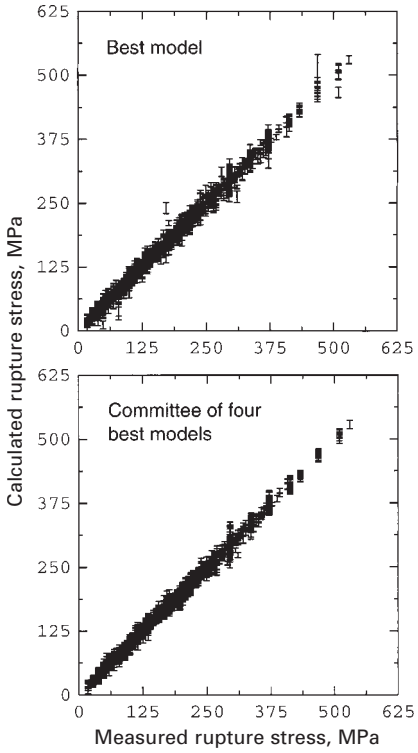

5 Plots of estimated *v.* measured creep rupture strength for the best single model and best committee of models

complexity it is necessary to examine how the model generalises on previously unseen data in the test data set using the test error. The latter is defined as

$$T_{en} = 0{\cdot}5 \sum_n (y_n - t_n)^2 \quad . \quad . \quad . \quad . \quad . \quad . \quad . \quad . \quad . \quad . \quad . \quad (5)$$

where y_n is the set of predictions made by the model, and t_n the corresponding target (experimental) values previously unseen by the model. Figure 4*b* shows that the test error at first decreases but then begins to increase again as a function of the number of hidden units.

MacKay[7] has suggested that the mean prediction of a committee of the best models from the set illustrated in Fig. 4*b* can give more reliable results than the very best single model. This can be attempted by first ranking all the models in order of worsening test error and then forming a committee with the N top models where $N = 1, 2, \ldots$. The test error for each committee can be evaluated in order to select its optimum size. The committee test error is shown as a function of the size of its membership in Fig. 4*c* where it is seen that the four best models form a committee which gives better estimates than the single best model.

Having chosen this committee, its four members were retrained on all the available data (test and training), in each case beginning with the weights obtained with just the training data. The retrained committee was used for all further work. Figure 5 shows a comparison between the predictions of the single best model and that of the committee after retraining each model on the entire data set. Consistent with the reduction in the test error illustrated in Fig. 4*c*, it is evident that the committee model outperforms the single best model.

Trends

It is useful to study the behaviour of the model for the two classic steels designated 2·25Cr–1Mo and 10CrMoW. The 2·25Cr–1Mo steel is a well established bainitic steel

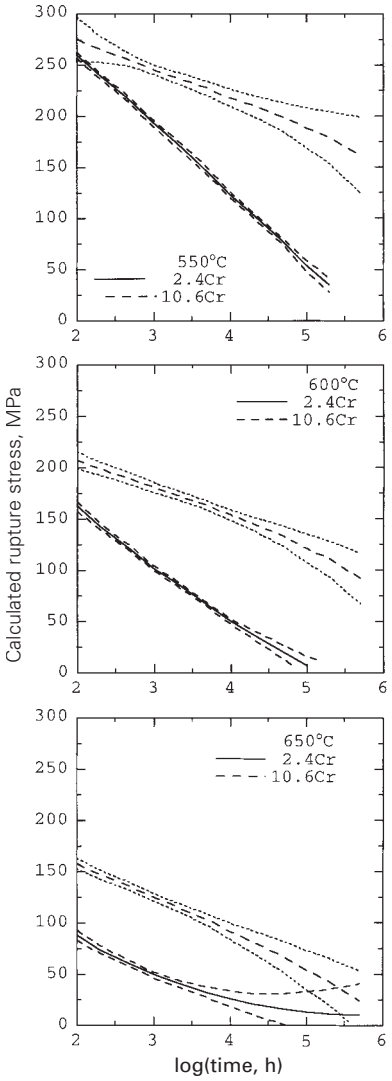

6 Calculated rupture strength as function of time at a variety of test temperatures: detailed compositions of the two steels are given in Table 2; the bands around each curve represent $\pm 1\sigma$ error bounds

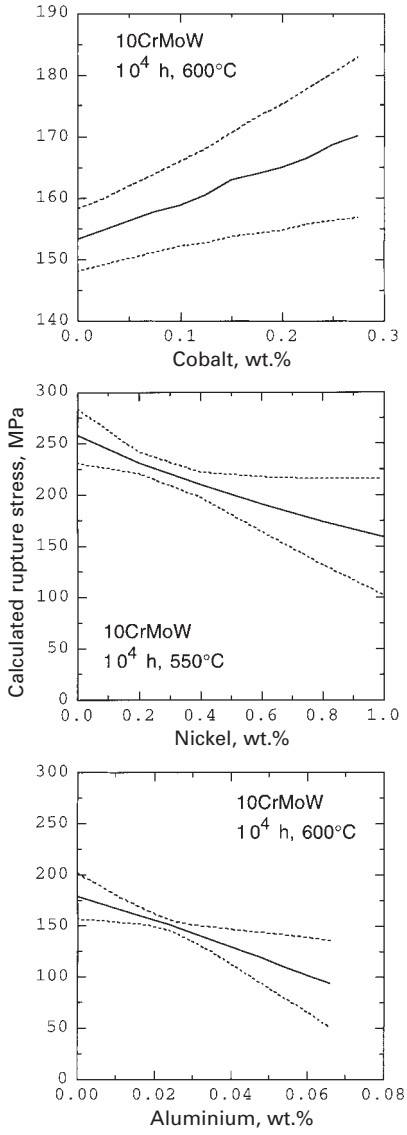

7 Calculated rupture strength for 10^4 h at indicated temperatures as function of *a* cobalt concentration; *b* nickel concentration; and *c* aluminium concentration in 10CrMoW steel: parameters are listed in Table 2; bands around each curve represent $\pm 1\sigma$ error bounds

designed for a maximum operating temperature of 565°C in power plant whereas the 10CrMoW steel is a more recent martensitic steel for use at higher temperatures. The typical set of inputs for these alloys is listed in Table 2. Although the calculations to be presented here are based on the neural network model, that model is not used in isolation when developing new alloys, as seen in the next section. The neural network modelling is supplemented with thermodynamic calculations to ensure the ability of the steel to become fully austenitic, and kinetic theory which estimates the evolution of carbides and Laves phases.

Figure 6 shows calculated curves of the stress rupture stress as a function of time at 550, 600, and 650°C. The model correctly reflects the better creep resistance of the 10CrMoW alloy at all temperatures. Modern design requires that the steel should be able to support a stress of 100 MPa at 100 000 h. This is achieved by the 10CrMoW steel at 600°C though neither would be adequate at the higher temperature of 650°C. Another feature of Fig. 6 is that the error bars for the 2·25Cr–1Mo steel are much smaller than for the 10CrMoW. This is because of the greater quantity of 2·25Cr–1Mo measurements in the data set since the steel has been used for nearly 60 years. Also it can be seen that the error bars get larger at long rupture times where the data are also sparse for both steels. The illustrations following Fig. 6 focus on the 10CrMoW steel which is more interesting from the point of view of the design of new alloys. Although changes in each of the input variables have been examined, only those trends which are significant are presented here.

Cobalt provides solid solution strengthening so the trend illustrated in Fig. 7 is reasonable. Cobalt is sometimes added in order to reduce the delta ferrite in the 10Cr type steels. However, phase diagram calculations using MTDATA[37] have shown that the steel becomes fully austenitic beyond about 1200 K. The effect of cobalt in those alloys where delta ferrite does form may therefore be larger since the ferrite is a soft phase compared with tempered martensite. The calculations for nickel are presented for the lower temperature of 550°C because those for 600°C had very large error bars making the trend unrecognisable (presumably because of a lack of data in that region of input space or because the data available are noisy). The deterioration in the rupture strength with increasing nickel concentration is well known although the metallurgical explanation is as yet missing. Strang and Vodarek[38] have suggested that the nickel stabilises the M_6X precipitates which coarsen rapidly and become ineffective as impediments to dislocation motion. Aluminium

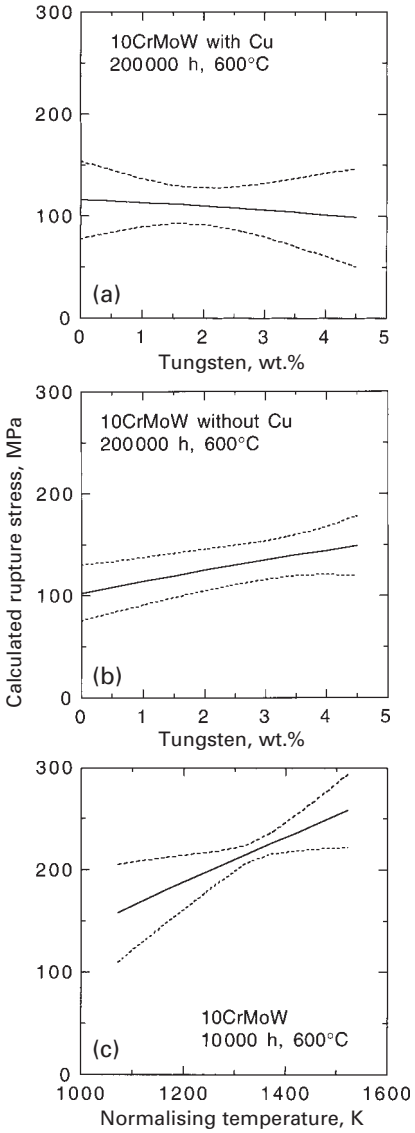

8 Calculated creep rupture strength for 10CrMoW steel showing combined effect of tungsten and copper, and of normalising temperature for treatment time of 2 h: bands around each curve represent $\pm 1\sigma$ error bounds

is detrimental in the 10CrMoW steel because it getters nitrogen in the form of coarse AlN, thereby reducing the precipitation of VN and NbN which are important in resisting creep deformation.[39]

Tungsten is known for its propensity to form Laves phase after very long times at high temperature. This is usually regarded as an undesirable phase because its nucleation rate is so small that the few particles that do form are coarse and hence of little use from the point of view of strength. The precipitation of Laves phase also leads to decrease in solid solution strengthening by reducing the amount of tungsten in solid solution.[40,41] Long term stress rupture calculations are presented in Fig. 8*a* for the 10CrMoW steel which also happens to contain a significant concentration of copper (0·86 wt-%, Table 2). It is seen that there may be a slight deterioration in the 200 000 h stress rupture strength at 600°C. Copper is known to promote the nucleation of Laves phase.[42] Calculations for the same alloy and identical circumstances but with the copper removed are illustrated in Fig. 8*b*. The strength now increases with the tungsten content presumably because the nucleation of Laves phase becomes more difficult.

The effect of the normalising temperature is illustrated in Fig. 8*c*; the improvement in the stress rupture strength

Table 2 The standard set of input parameters for two alloys used to examine trends predicted by the neural network

Parameter	2·25Cr–1Mo	10CrMoW
Normalising temperature, K	1203	1338
Duration, h	6	2
Cooling rate	WQ*	AC*
Tempering temperature, K	908	1043
Duration, h	6	4
Cooling rate	AC*	AC*
Annealing temperature, K	873	1013
Duration, h	2	4
Cooling rate	AC*	AC*
Chemical composition, wt-%		
C	0·15	0·12
Si	0·21	0·05
Mn	0·53	0·64
P	0·012	0·016
S	0·012	0·001
Cr	2·4	10·61
Mo	1·01	0·44
W	0·01	1·87
Ni	0·14	0·32
Cu	0·16	0·86
V	0·01	0·21
Nb	0·005	0·01
N	0·0108	0·064
Al	0·018	0·022
B	0·0003	0·0022
Co	0·05	0·015
Ta	0·0003	0·0003
O	0·01	0·01
Re	0·0003	0·0003

* WQ water quenched, AC air cooled.

is consistent with an increasing dissolution of precipitate phases as the temperature is raised. The accompanying increase in the austenite grain size is known to be beneficial since creep damage is usually focused at these grain boundaries.[43] Note that the narrow range of normalising temperatures over which the model has a high confidence is a reflection of the range of data available for steels of this class.

It has been demonstrated that wherever significant trends are observed, they can be shown to be consistent with

Table 3 Input parameters for the 10CrMoW steel and predicted design parameters for steels A and B

Parameter	10CrMoW	Steel A	Steel B
Normalising temperature, K	1338	1473	1453
Duration, h	2	2	2
Cooling rate	AC*	AC*	AC*
Tempering temperature, K	1043	1073	1073
Duration, h	4	4	4
Cooling rate	AC*	AC*	AC*
Annealing temperature, K	1013	1013	1013
Duration, h	4	4	4
Cooling rate	AC*	AC*	AC*
Chemical composition, wt-%			
C	0·12	0·12	0·13
Si	0·05	0	0
Mn	0·64	0·48	0·5
P	0·016	0·0016	0·0016
S	0·001	0·001	0·001
Cr	10·61	9	8·7
Mo	0·44	0·75	0·3
W	1·87	3	3
Ni	0·32	0	0
Cu	0·86	0	0
V	0·21	0·21	0·21
Nb	0·01	0·01	0·01
N	0·064	0·064	0·064
Al	0·022	0	0
B	0·0022	0·008	0·008
Co	0·015	1·25	0
Ta	0·0003	0·0003	0·0003
O	0·01	0·01	0·01
Re	0·0003	0·0003	0·0003

* AC air cooled.

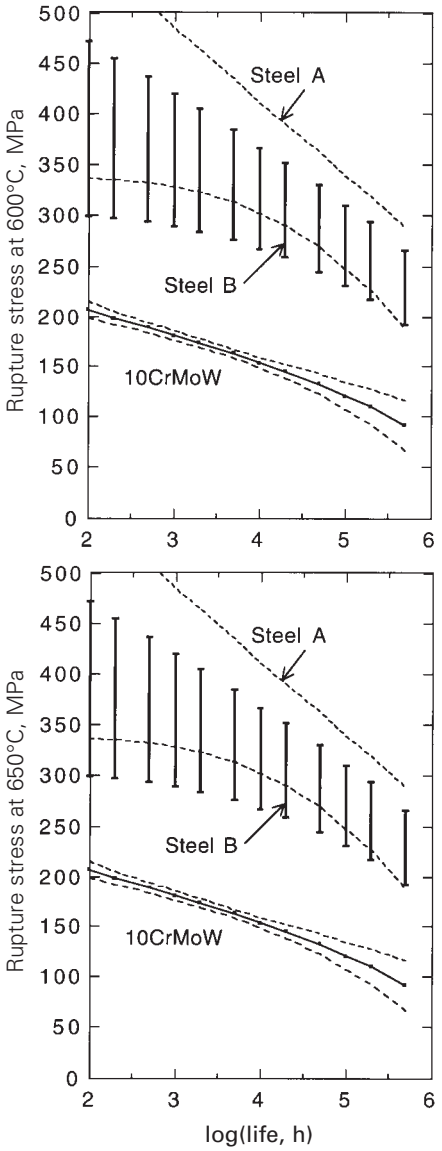

9 Calculated creep rupture strength as function of time at 600 and 650°C for standard 10CrMoW steel and steel A: bands round each curve represent $\pm 1\sigma$ error bounds

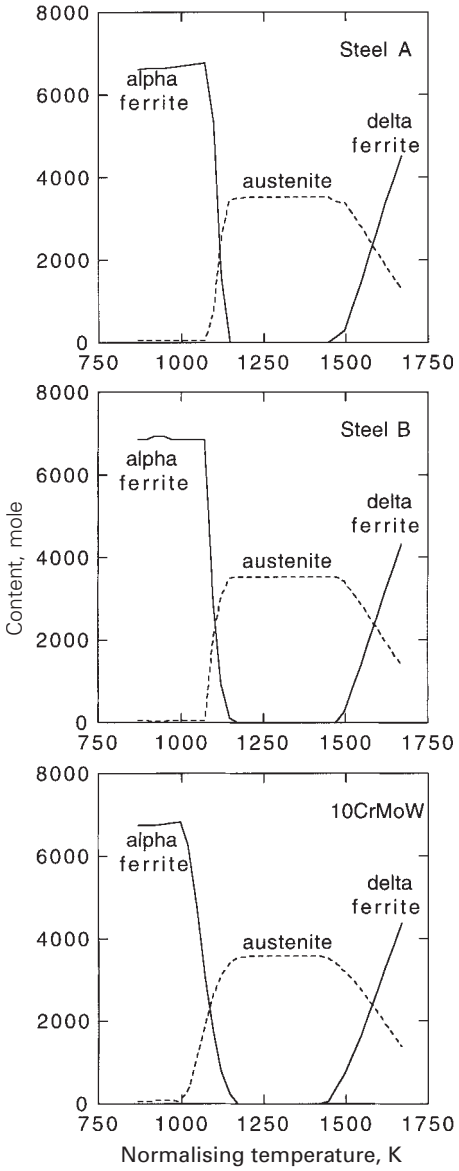

10 Calculated phase quantities for steel A, steel B, and standard 10CrMoW alloy as functions of temperature: phase quantities are moles of unit cells; austenite has four atoms per unit cell whereas ferrite has two

what is expected from physical metallurgy. However, it is emphasised that the neural network method was used in the first place because of the complexity of the problem. The number of variables is large and there are interactions between the variables. It is not possible to visualise these multidimensional interactions and so it is unlikely that the model can ever be tested completely.

Proposal for novel steels

The model is now used to propose some novel alloys with stress rupture properties which are predicted to be better than existing steels. The procedure involves a systematic search of the input space focusing on directions which lead to a maximisation of certainty, i.e. minimisation of error. The detailed trends investigated are too voluminous to report here but have been documented in an internal report. The calculations involved the modification of the standard 10CrMoW steel (Table 2) so all the results are compared against that alloy. The first attempt led to the design of alloy A (Table 3) but its long term properties at 650°C just fail to meet the 100 MPa requirement (Fig. 9). Changes were therefore made to improve both the mean long term properties and the certainty in their prediction, by reducing the cobalt, chromium, and molybdenum concentrations.

The new alloys do not contain any silicon, aluminium, nickel, or copper, all of which were demonstrated earlier to lead to a deterioration in the creep rupture stress. The boron concentration is kept smaller than the maximum in the database, primarily to reduce the uncertainty in the predictions. There is an increase in the normalising temperature, and reductions in the manganese and chromium concentrations together with an increase in the level of tungsten.

The neural network calculations were done in conjunction with phase diagram calculations using the MTDATA program,[37] and kinetic predictions using the methodology described elsewhere.[44–46] The phase diagram calculations confirmed that there is a wide temperature range about the proposed normalising temperature, over which only austenite is the stable phase (Fig. 10). This is important in order to avoid the retention of delta ferrite in the microstructure.

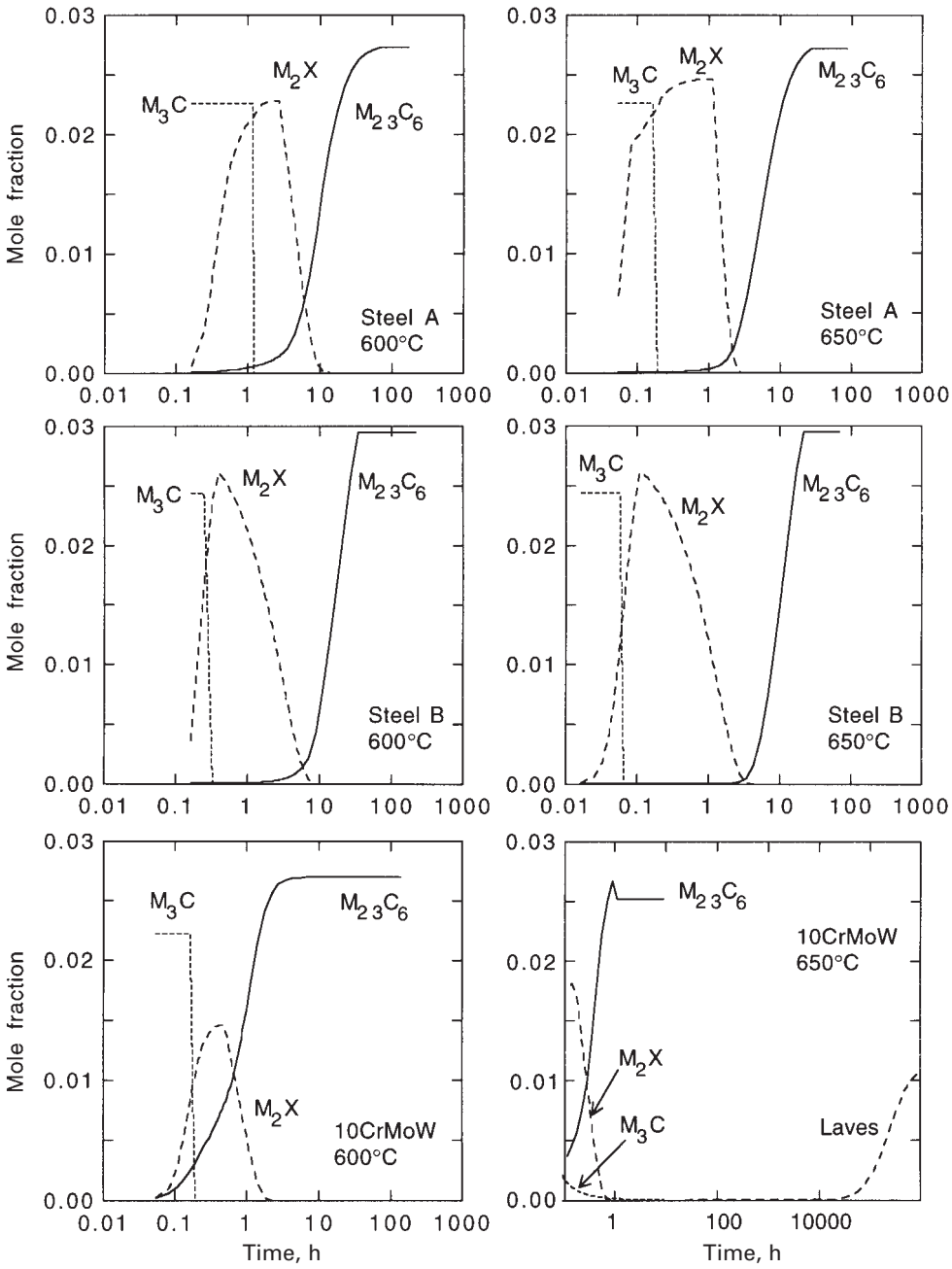

11 Calculated variation in fraction of precipitates as function of time and temperature for steel A, steel B, and standard 10CrMoW steel: note that scale on 10CrMoW 650°C graph differs from the rest of the plots

Table 4 shows the calculated equilibrium fractions of $M_{23}C_6$ and Laves phase in each of the steels. Note that other carbides including M_2C, M_6C, M_7C_3, and M_3C were included in the calculations but were found to be metastable relative to the equilibrium structure listed in Table 4. To assess whether the steels are actually susceptible to Laves phase formation requires kinetic calculations. There has been progress recently in the calculation of precipitation reactions in power plant steels on the basis of thermodynamic data and kinetic theory.[44–46]

Table 4 Calculated equilibrium mole fractions of phases

		Temperature, °C		
Steel	Phase	600	650	700
10CrMoW	$M_{23}C_6$	0·0269	0·0269	0·0268
	Laves	0·0113	0·0079	0·0024
Steel A	$M_{23}C_6$	0·0273	0·0273	0·0271
	Laves	0·0264	0·0234	0·0188
Steel B	$M_{23}C_6$	0·0294	0·0294	0·0292
	Laves	0·020	0·0165	0·0113

The calculations using this method are presented in Fig. 11, which shows that Laves phase only occurs in the 10CrMoW steels at the very late stages of annealing at 650°C. Steels A and B were not found to exhibit Laves phase precipitation, at least after 10^6 h at 600 or 650°C. This is because they contain larger fractions of M_2X precipitation, which reduces the driving force that is available for the subsequent formation of Laves phase.

Finally, discussions with manufacturers and users of power plant indicate that the proposed steels are realistic from a manufacture and processing point of view. It is interesting that we have drawn on a large published database interpreted using a neural network, kinetic theory, thermodynamic theory, and experience in order to reach the proposed alloys. The actual predictions remain to be tested.

Conclusions

A neural network has been used to model the creep rupture strength of bainitic and martensitic electric power plant steels based on alloys in the composition range Fe–2·25Cr–1Mo to Fe–(9–12)Cr, as a function of chemical composition, heat treatment, and time at temperature. This has been combined with thermodynamic and kinetic calculations, together with metallurgical experience, to propose two new alloys. These alloys should in theory have excellent stress rupture properties, but the predictions remain to be tested experimentally.

Acknowledgements

The authors are grateful to Professor Alan Windle for the provision of laboratory facilities at the University of Cambridge, to the Ecole Polytechnique (Paris), EPSRC, JRDC (Japan), The Royal Society, IHI (Japan) and Sollac (France) for assisting this work via a variety of mechanisms.

References

1. R. W. EVANS and B. WILSHIRE: 'Creep of metals and alloys'; 1985, London, The Institute of Materials.
2. F. B. PICKERING: in 'Microstructural development and stability in high chromium ferritic power plant steels', (ed. A. Strang and D. J. Gooch), 1–30; 1997, London, The Institute of Materials.
3. D. J. C. MacKAY: *Neural Comput*., 1992, **4**, 415–447.
4. D. J. C. MacKAY: *Neural Comput*., 1992, **4**, 448–472.
5. D. J. C. MacKAY: *Network: Comput. Neural Syst*., 1995, **6**, 469–505.
6. D. J. C. MacKAY: *Trans. Am. Soc. Heat., Refrig. Air Cond. Eng*., 1994, **100**, 1053–1062.
7. D. J. C. MacKAY: in 'Mathematical modelling of weld phenomena', (ed. H. Cerjak and H. K. D. H. Bhadeshia), 359; 1997, London, The Institute of Materials.
8. E. C. BAIN: 'Alloying elements in steel'; 1939, Cleveland, OH, American Society for Metals.
9. National Research Institute for Metals: *NRIM Creep Data Sheets*, 1991, **36A**; 1986, **3B**; 1994, **13B**; 1979, **10A**; 1981, **19A**.
10. F. MASUYAMA and M. OHGAMI: 'Aspects of high temperature deformation and fracture in crystalline materials', 325–332; 1993, Sendai, Japan Institute of Metals.
11. F. ABE and S. NAKAZAWA: *Metall. Trans. A*, 1992, **23A**, 3025–3034.
12. V. SKLENIČKA, K. KUCHAŘOVA, A. DLOUGHÝ, and J. KREJČÍ: in 'Materials for advanced power engineering', Part 1, 435–444; 1994, Dordrecht, Kluwer Academic Publishers.
13. F. MASUYAMA and T. YOKOYAMA: in 'Materials for advanced power engineering', Part 1, 301–308; 1994, Dordrecht, Kluwer Academic Publishers.
14. L. KUNZ, P. LUKAŠ, and V. SKLENIČKA: in 'Materials for advanced power engineering', Part 1, 445–452; 1994, Dordrecht, Kluwer Academic Publishers.
15. T. FUJITA: in 'Future ferrite steels for high-temperature service: new steels for advanced plant up to 620°C', (ed. E. Metcalfe), 190–200; 1995, Palo Alto, CA, EPRI.
16. B. S. GREENWELL and J. W. TAYLOR: in Conference Series C386/041, 283–296; 1990, London, The Institution of Mechanical Engineers.
17. J. HALD: in 'Future ferrite steels for high-temperature service: new steels for advanced plant up to 620°C', (ed. E. Metcalfe), 152–173; 1995, Palo Alto, CA, EPRI.
18. G. A. HONEYMAN: in 'Future ferrite steels for high-temperature service: new steels for advanced plant up to 620°C', (ed. E. Metcalfe), 70–83; 1995, Palo Alto, CA, EPRI.
19. F. BRÜHL, K. HAARMANN, G. KALWA, H. WEBER, and M. ZSCHAU: *VGB Kraftwerkstechnik*, 1989, **69**, 1064–1080.
20. P. J. GROBNER and W. C. HAGEL: *Metall. Trans. A*, 1980, **11A**, 633–642.
21. H. NAOI, H. MIMURA, M. OHGAMI, H. MORIMOTO, T. TANAKA, Y. YAZAKI, and T. FUJITA: in 'Future ferrite steels for high-temperature service: new steels for advanced plant up to 620°C', (ed. E. Metcalfe), 8–29; 1995, Palo Alto, CA, EPRI.
22. M. MORINAGA, R. HASHIZUME, and Y. MURATA: in 'Materials for advanced power engineering', Part 1, 319–328; 1994, Dordrecht, Kluwer Academic Publishers.
23. V. K. SIKKA, M. G. COWGILL, and B. W. ROBERTS: in 'Proceedings of topical conference on ferritic alloys for use in nuclear technologies', 413–423; 1984, Warrendale, PA, TMS-AIME.
24. M. L. SHAW, T. B. COX, and W. C. LESLIE: *J. Mater. Energy Syst*., 1987, **8**, 347–355.
25. Y. TSUCHIDA, R. YAMABA, K. TOKUNO, K. HASHIMOTO, T. OGAWA, and T. TAKEDA: Internal report, Nippon Steel Corp., Tokyo, Japan, 1990.
26. C. COUSSEMENT, M. DE WITTE, A. DHOOGE, R. DOBBELAERE, and E. VAN DER DONCKT: *Rev. Soudure*, 1990, **1**, 58–63.
27. H. MASUMOTO, H. NAOI, T. TAKAHASHI, S. ARAKI, T. OGAWA, and T. FUJITA: in 'EPRI 2nd Conference', 1988, 40.3–40.10; 1988, Palo Alto, CA, EPRI.
28. V. K. SIKKA and R. H. BALDWIN: 'Data package for modified 9Cr1Mo alloy, update', Internal report, Oak Ridge National Laboratories, Oak Ridge, TN, USA, 1987.
29. A. ISEDA, M. KUBOTA, Y. HAYASE, S. YAMAMOTO, and K. YOSHIKAWA: *Sumitomo Search*, 1988, **36**, 17–29.
30. J. ORR and D. BURTON: in 'Materials for advanced power engineering', Part 1, 263–280; 1994, Dordrecht, Kluwer Academic Publishers.
31. Internal report, Nippon Kokan, Chiba, Japan, 1987.
32. T. FUJITA, K. ASAKURA, T. SAWADA, T. TAKAMATSU, and Y. OTOGURO: *Metall. Trans. A*, 1981, **12A**, 1071–1079.
33. T. FUJITA and N. TAKAHASHI: *Trans. ISIJ*, 1979, **18**, 269–278.
34. A. HIZUME, Y. TAKEDA, H. YOKOTA, Y. TAKANO, A. SUZUKI, S. KINOSHITA, M. KOHNO, and T. TSUCHIYAMA: in 'Advanced materials technology '87', (ed. R. Carson *et al.*), 143–151; 1987, Corvina, CA, SAMPE.
35. K. KUWABARA, A. NITTA, T. OGATA, and S. SUGAI: in 'Advanced materials technology '87', (ed. R. Carson *et al.*), 153–162; 1987, Corvina, CA, SAMPE.
36. K. HAARMANN and G. P. KALWA: in 'Advanced materials technology '87', (ed. R. Carson *et al.*), 267–273; 1987, Corvina, CA, SAMPE.
37. 'MTDATA (Metallurgical and thermochemical databank)', National Physical Laboratory, Teddington, Middx, UK 1989.
38. A. STRANG and V. VODAREK: *Mater. Sci. Technol*., 1996, **12**, 552–556.
39. V. FOLDYNA, Z. KUBON, V. JAKOVOVA, and V. VODAREK: in 'Microstructural development and stability in high chromium power plant steels', (ed. A. Strang and D. J. Gooch), 74–92; 1997, London, The Institute of Materials.
40. J. HALD and Z. KUBOŇ: in 'Microstructural development and stability in high chromium power plant steels', (ed. A. Strang and D. J. Gooch), 159–178; 1997, London, The Institute of Materials.
41. J. D. ROBSON and H. K. D. H. BHADESHIA: in 'Microstructural development and stability in high chromium power plant steels', (ed. A. Strang and D. J. Gooch), 179–208; 1997, London, The Institute of Materials.
42. M. SCHWIND, M. HÄTTERSTRAND, and H.-O. ANDRÉN: Internal COST 501 Report, Chalmers University, Gothenburg, Sweden, 1996.
43. H. E. EVANS: 'Mechanisms of creep fracture'; 1984, Barking, Elsevier Applied Science.
44. J. D. ROBOSON and H. K. D. H. BHADESHIA: *Mater. Sci. Technol*., 1997, **13**, 631–639.
45. J. D. ROBSON and H. K. D. H. BHADESHIA: *Mater. Sci. Technol*., 1997, **13**, 640–644.
46. J. D. ROBSON and H. K. D. H. BHADESHIA: *Calphad*, 1996, **20**, 447–460.